Ultramicroscopy 111 (2011) 1366–1369

Contents lists available at ScienceDirect

Ultramicroscopy

journal homepage: www.elsevier.com/locate/ultramic

Broadband *nano*dielectric spectroscopy by means of amplitude modulation electrostatic force microscopy (AM-EFM)

G.A. Schwartz [a,*], C. Riedel [a,b,c], R. Arinero [c], Ph. Tordjeman [d], A. Alegría [a,e], J. Colmenero [a,b,e]

[a] Centro de Física de Materiales CSIC-UPV/EHU, Materials Physics Center MPC, Paseo Manuel de Lardizabal 5, 20018 San Sebastián, Spain
[b] Donostia International Physics Center, Paseo Manuel de Lardizabal 4, 20018 San Sebastián, Spain
[c] Institut d'Electronique du Sud (IES), Université Montpellier II, 34095 Montpellier Cedex, France
[d] IMFT, Université de Toulouse, CNRS, 1 Allée du Professeur Camille Soula, 31400 Toulouse, France
[e] Departamento de Física de Materiales UPV/EHU, Facultad de Química, 20080 San Sebastián, Spain

ARTICLE INFO

Article history:
Received 17 January 2011
Received in revised form
19 April 2011
Accepted 2 May 2011
Available online 19 May 2011

Keywords:
Amplitude modulation AFM
Dielectric spectroscopy
Polymers
Thin films
Heterogeneous materials

ABSTRACT

In this work we present a new AFM based approach to measure the local dielectric response of polymer films at the nanoscale by means of Amplitude Modulation Electrostatic Force Microscopy (AM-EFM). The proposed experimental method is based on the measurement of the tip–sample force via the detection of the second harmonic component of the photosensor signal by means of a lock-in amplifier. This approach allows reaching unprecedented broad frequency range ($2–3\times10^4$ Hz) without restrictions on the sample environment. The method was tested on different poly(vinyl acetate) (PVAc) films at several temperatures. Simple analytical models for describing the electric tip–sample interaction semi-quantitatively account for the dependence of the measured local dielectric response on samples with different thicknesses and at several tip–sample distances.

1. Introduction

Standard broadband dielectric spectroscopy (BDS) is a well known, established and extremely useful technique to follow the molecular dynamics of bulk materials containing polar entities over a huge frequency range (10^{-5}–10^{12} Hz) under different temperature, pressure and environment conditions (see for example [1]). Thus, several molecular processes in the bulk, at very different time scales, can be observed by means of standard BDS. In spite of these exceptional characteristics and features, standard BDS can only measure the macroscopic average dielectric response, which means that no spatial resolution can be achieved. This is an important limitation that seriously restricts the use of standard BDS to investigate heterogeneous or nano-structured systems, where spatial resolution is essential. During the last decade, some attempts to measure the local dielectric response at nano-metric scale were carried out by different groups. Most of the explored methods consist to adapt existing AFM facilities to accomplish local measurements of different quantities (capacitance [2,3], DC [4–6] and AC [7–11] electrostatic force gradients) that can be related by means of appropriated models with the dielectric response. However, these methods present some important limitations: some of them work under vacuum whereas others only account for the static dielectric permittivity or measure its frequency response over a limited frequency range.

In this work we present a novel approach, based on amplitude modulation electrostatic force microscopy (AM-EFM) to measure the local dielectric response of polymer films with both nanometric lateral resolution and broad frequency band. This method can be easily implemented on standard AFM without any special instrumentation and, especially important, under room conditions or controlled atmosphere as well. Moreover, this simple method allows performing *nano*dielectric spectroscopy with an unprecedented broad frequency range, which could eventually be extended up to six decades. Although we use similar AFM setup than that used in some previous works, the main point of our approach is related with the fact that we directly analyze the response on the photosensor (i.e. the force signal) instead of measuring cantilever's resonance frequency or phase (i.e. force gradient signal) or the tip–sample capacitance. Advantages and limitations of this approach will be discussed.

2. Principles of AM-AFM operation

The basic idea of the method is to measure by means of an AFM the electric force between the tip and an insulating sample when an AC voltage is applied between the tip and a conductive

* Corresponding author. Tel.: +34 943 01 8807; fax: +34 943 01 5600.
E-mail address: schwartz@ehu.es (G.A. Schwartz).

0304-3991/$ - see front matter © 2011 Elsevier B.V. All rights reserved.
doi:10.1016/j.ultramic.2011.05.001

substrate supporting the sample. The time dependence of the force can be obtained from the photosensor signal and then related with the dielectric permittivity of the sample using an appropriated model. By measuring the dielectric response at large enough values of the tip–sample distance, the repulsive contact force as well as van der Walls forces can be neglected. Therefore, under these conditions, the force between the tip and the sample is purely electrostatic and is given by $F=1/2(\partial C/\partial z)V^2$, where V is the voltage between the tip and the substrate and C the cantilever-tip–sample capacitance. When a sinusoidal voltage ($V=V_0\sin(\omega_e t)$) is applied to the probe, the 2ω component of the electrostatic force is given by $F_{2\omega}=1/4(\partial C/\partial z)V_0^2\cos(2\omega_e t)$.

The signal of the photodiode A_p gives direct access to the electrostatic force. For small forces we can assume linearity and therefore the force is given by $F=A_p\chi k_c$, where k_c is the stiffness of the cantilever and χ is a factor of proportionality (expressed in nm/V) between the signal of the photodiode (in volts) and the deflection of the cantilever (in nm). χ can be experimentally determined by means of a force–distance curve recorded on a stiff sample. Thus, by measuring with a lock-in amplifier the second harmonic of the signal from the photodiode we get:

$$A^*_{p,2\omega_e}=(\chi k_c)^{-1}F^*_{p,2\omega_e}=V_0^2(4\chi k_c)^{-1}(\partial C^*/\partial z) \quad (1)$$

where * indicates complex quantities and the capacity (C) contains the information about the dielectric properties of the polymer film.

3. Experimental details

3.1. Sample preparation

In order to test the proposed method we measured the dielectric response on different poly(vinyl acetate) (PVAc$-[C_4H_6O_2]_n-M_w=$ 33,200 g/mol) films. The samples were obtained by spin coating toluene solutions of the polymer (with different concentrations) over a gold sputtered glass electrically grounded to the sample holder. The samples were dried under room conditions for 2 h and then at 120 °C under vacuum for another 2 h. A scratch with a sharp tool was made on each sample in order to evaluate the polymer thickness from the profile measured by AFM.

3.2. EFM measurements

The experiments were performed on a Veeco Multimode AFM with a Nanoscope V controller. We used SCM-PIT coated tips having a typical free oscillation frequency (f_o) of 75 kHz and stiffness (k_c) of 4 Nm^{-1}. The experiments were performed at different temperatures between room temperature and 70 °C (being the glass transition temperature of PVAc ($T_g=$) 38 °C). To measure the local dielectric response of the sample by means of the AFM we used the so-called double pass method. In this way, we keep the tip oscillating in the Tapping® mode, sensing the topography of the sample, and then the tip is retracted at a given constant height (lift scan) to maintain the tip at a fixed distance from the sample surface. During the lift scan an AC voltage is applied on the tip and the second harmonic of the photosensor signal is then measured by means of a lock-in amplifier. Finally, we subtracted from the phase of the second harmonic of the photosensor signal measured at different temperatures, the corresponding value of the phase measured on the same sample well below T_g (where negligible frequency dependent contributions from PVAc are expected). Thus, the phase measured at low temperatures serves as a reference signal to be subtracted in order to compensate the instrumental frequency response from the measurement system. In this way, we put on the real part of the response, all the parasite and non-controlled contributions from the cantilever and the rest of the experimental setup. Thus, the obtained phase difference only contains information about the frequency response of the material under investigation.

Finally, we would like to discuss an important point concerning to temperature control and measurement. In our experimental setup, we heat the sample from the bottom and measure the temperature just below the sample holder. This method produces a temperature gradient between the heater and the surface of the sample, which means the last is actually at a lower (and non-precisely known) temperature. Thus, the temperature uncertainty in our experimental setup is bigger than the reported difference between bulk and local dynamics (1–3 K). Although the temperature precision is not a crucial point for the purposes of the present manuscript, we are currently working on a new system for improving both temperature control and measurement.

4. Results and discussion

Fig. 1 shows the phase difference, obtained as explained before, as a function of the frequency at several temperatures for a PVAc film 250 nm thick. The phase difference follows a temperature–frequency dependence qualitatively similar to that observed for the macroscopic loss dielectric permittivity for bulk PVAc [12–14]. The most relevant observation emerging from this figure is the broad frequency range (more than four decades) experimentally accessible. This is in fact the broadest range obtained so far by means of AFM based approaches. Previous frequency modulation EFM experiments (FM-EFM) based on the detection of AC force gradients [7–10] were limited to cover only three decades in frequency due to the response of the first-order filter behaviour of the photosensor [15]. In this work we restricted the high frequency limit to about 37 kHz (which is half the resonance frequency of the cantilever) because we observed that the reference phase reached extremely high values increasing the uncertainties of the measured response. Using stiffer cantilevers it is expected to increase the high frequency range although, at the same time, decreasing the sensitivity. On the other hand, the low frequency limit is imposed by the thermal drift of the system. At low frequencies, the required time to measure the dielectric response increases and therefore any effect due to the thermal drift of the system will introduce bigger uncertainties. By improving the thermal stabilization of the system it would be possible to

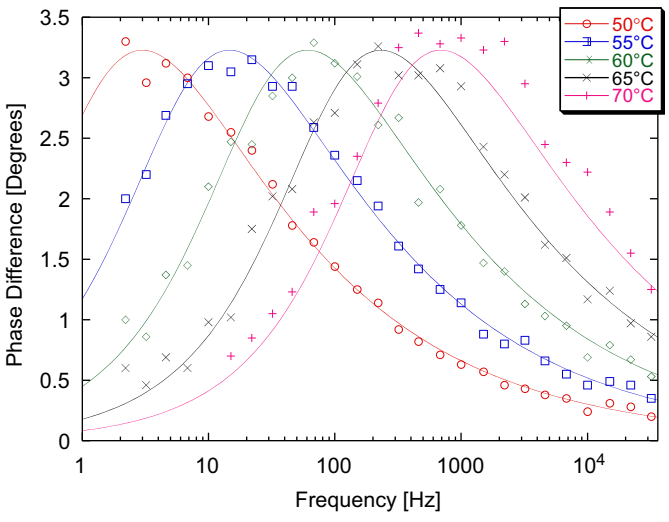

Fig. 1. Phase difference as a function of frequency at several temperatures for PVAc. Note the broad frequency range. The lines are guides for the eyes.

further decrease the low frequency limit. Taking into account these considerations it would be possible to increase the frequency range up to around six decades. We note that this would be comparable to the typical range used for bulk measurements.

We will turn now to discuss about how the obtained phase difference is related with the expected signal from the polymer and how the film thickness and the tip–sample distance affect the measured response. Fig. 2a shows the experimental phase difference measured at 60 °C for PVAc at constant tip–sample distance and different thicknesses. We observe a clear increment of the amplitude with increasing film thickness. On the contrary, the peak position seems to be not (or very slightly) affected by the thickness. On the other hand, Fig. 3a shows the experimental phase difference measured at 60 °C for PVAc at constant thickness and different tip–sample distances. As in the previous case, we observe an increment of the phase difference with decreasing tip–sample distance. In addition, we observe here a more pronounced shift of the peak maximum towards lower frequencies with decreasing tip–sample distance.

In order to analyze the obtained results we will use a previously proposed model to describe the tip–sample interaction. Although this simple model is valid under certain approximations and could not be strictly applicable to our whole set of experiments, it is nevertheless a way to gain insight into the origin of the observed effects. The model, proposed by Fumagalli et al. [2], estimates the apex capacitance based on the dihedral approximation and was also tested by finite numerical simulations (see Ref. [2] for more details). Thus, we can write the apex capacitance as a function of the sample permittivity (ε), tip–sample distance (z), film thickness (h) and tip geometry (apex radius (R) and cone angle (θ)) as $C_{ap}=2\pi\varepsilon_0 R\ln(1+R(1-\sin\theta_0)/(z+h/\varepsilon))$. Then, by derivating this expression results in:

$$\frac{\partial C^*_{ap}}{\partial z}=\frac{2\pi\varepsilon_0 R^2}{h^2}\left[\frac{(\varepsilon^*)^2(1-\sin\theta_0)}{(1+\varepsilon^* z/h+\varepsilon^* R/h(1-\sin\theta_0))(\varepsilon^* z/h+1)}\right] \quad (2)$$

where ε^* is the complex dielectric permittivity accounting for the frequency dependent effect on the sample response. We have modelled in Eq. (2) the complex dielectric permittivity using the Havriliak–Negami (HN) function $\varepsilon^*(\omega)=\varepsilon_\infty+\Delta\varepsilon(1+(i\omega\tau)^\alpha)^{-\beta}$ (see Refs. [12,14] for more details) with the parameters that correspond to bulk PVAc at 60 °C. Measured signal $A^*_{p,2\omega_e}$ (see Eq. (1)) contains contributions not only from C^*_{ap} but also from

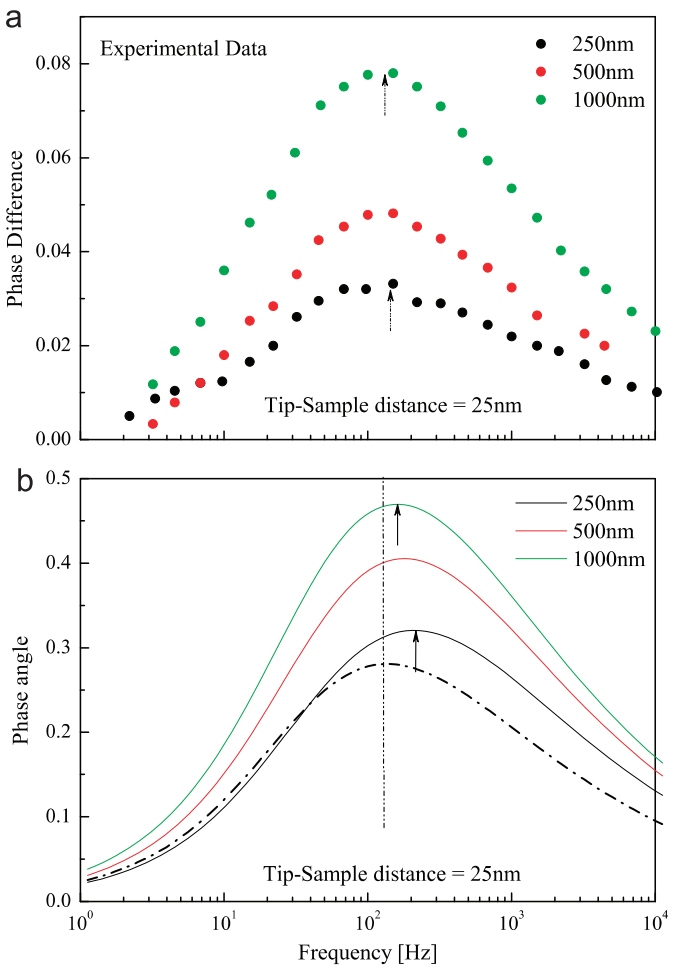

Fig. 2. (a) Experimental phase difference as a function of frequency at constant tip–sample distance for PVAc thin films with different thicknesses. (b) Calculated phase angle as a function of frequency at constant tip–sample distance for different sample thicknesses in terms of the model here analyzed. Thick dash dotted line represents the HN function used as input for both models. The vertical dotted line indicates the position of the maximum for this function. In both plots the arrows indicate the position of the maximum for each curve. The peak maximum slightly shifts to lower frequencies with increasing film thickness. The position of the peak maximum is always faster than the input.

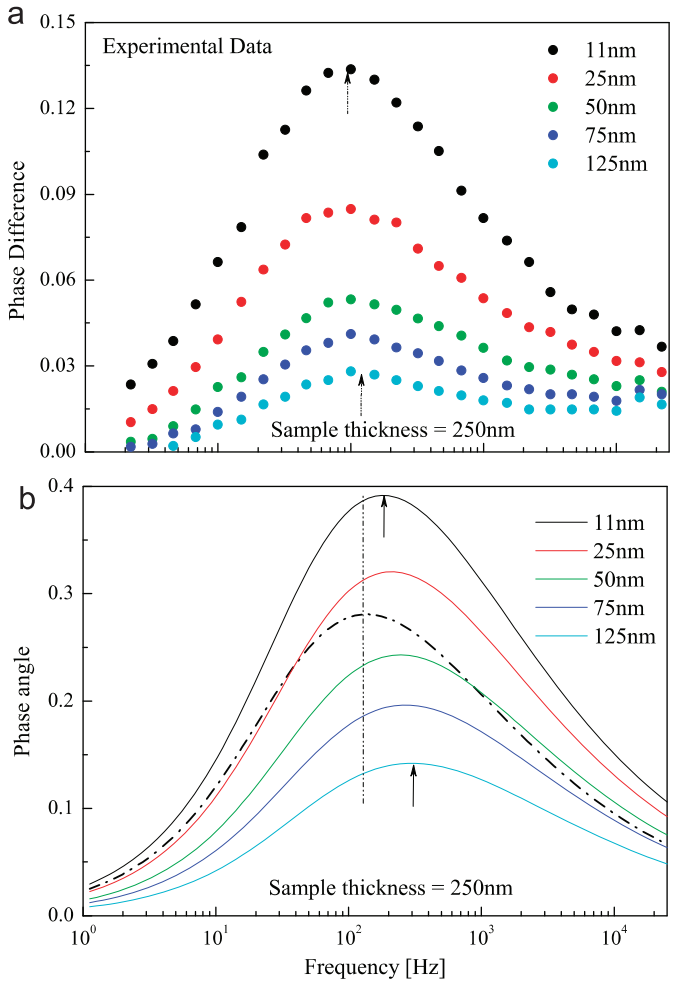

Fig. 3. (a) Experimental phase difference as a function of frequency at different tip–sample distances for PVAc thin films with constant thicknesses. (b) Calculated phase angle as a function of frequency at different tip–sample distances for PVAc thin films with constant thicknesses in terms of the model here analyzed. Thick dash dotted line represents the HN function used as input for both models. The vertical dotted line indicates the position of the maximum for this function. In both plots the arrows indicate the position of the maximum for each curve. The peak maximum shifts to lower frequencies with decreasing tip–sample distance. The position of the peak maximum is always faster than the input.

the so-called stray capacitance (C_{st}) in parallel with C^*_{ap}. Thus, C^*in Eq. (1) is given by $C^* = C^*_{ap} + C_{st}$. Note that, in order to use Eq. (1), the phase difference is calculated with respect to the measurement at room temperature (well below the glass transition temperature). In this way, the phase difference only contains contributions from C^*_{ap} but not from the stray capacitance (C_{st}) under the assumption that the influence of the polymer on C_{st} is negligible.

Finally, we have calculated the corresponding frequency dependence of Eq. (2) for different values of the film thickness (h) and tip–sample distance (z). Fig. 2b shows the calculated phase angle values at constant tip–sample distance and different thicknesses. The thick dash dotted line represents the dielectric loss corresponding to the HN function used as input. The vertical dotted line indicates the position of the maximum for this function. The negligible (or slightly) peak maximum shift to lower frequencies with increasing sample thickness observed in the experiments is well captured by the calculated curves. We also note that, for the model, the position of the peak maximum is always at slightly higher frequencies than for the input relaxation function and that both approach for thicker films. Fig. 3b shows the calculated phase angle at constant thickness and different tip–sample distances. Again, the thick dash dotted line represents the imaginary part of the HN function used as input. We also observe here a more pronounced shift of the peak maximum towards lower frequencies with decreasing tip–sample distance in agreement with the experiments although more prominent. Again, for all cases the calculated peak appears at higher frequencies than that of the input one. This faster equivalent relaxation time, in comparison with the input value, is in agreement with previously reported results using other AFM based measurements on thin films of PVAc [8,10]. Although these authors used different approaches, the reported faster local dynamics in the films could be, at least partially, more related with the experimental method used than being attributed to actual sample dynamics changes. In addition, as stated in previous works [7,8] and based on our own calculations [16], the probe volume (in the gradient mode) is about 40 nm in diameter and 20 nm in depth (although it depends on tip–sample distance) for a tip radius of about 30 nm. In the case of force mode, the probe volume is even deeper. This means that by means of EFM we are probing more near surface material but we have also important contributions from bulk-like behaviour. Taking this into account, gradient mode is more appropriated than force mode to probe small volumes (with lower bulk-like contributions). Therefore, smaller tips than those used so far are necessary to account for near surface dynamics. Only in this way we can increase sufficiently the relative contribution of the near surface polymer compared to the bulk one.

Finally, a careful analysis of Figs. 2 and 3 shows that the frequency shift of the peak maximum changes a little bit more with tip–sample distance than with sample thickness. These figures seem to indicate that measurements on thick samples and with small tip–samples distance would provide peak frequencies closer to the real response. It is worth to note that other even simpler model, based on a parallel plate capacitor description [8], provides essentially the same characteristics which evidences that the previous findings are not substantially determined by the choice of the model. In any case, although there is a good qualitative agreement between the experimental results and the calculated curves, it is clear that more reliable models for tip–sample interaction are needed for an accurate quantitative analysis.

5. Conclusions

In summary, we have presented a new approach to access the local dielectric response of thin films with nanoscale spatial resolution. The proposed method represents a substantial advance compared to other existing methods because it opens the way to experiments easier to implement with standard AFM under room conditions covering at the same time an unprecedented broad frequency range. In the near future, studies of the local dielectric response of biological or other soft matter materials should thus be possible. Numerical calculations, based on rather simple models to account for the tip–sample interaction, have shown to qualitatively describe the experimental results. This comparison indicates that the measured peak frequency is slightly higher than the expected one and this difference depends on the experimental details. This means that more precise models are still needed in order to provide quantification of the dielectric interaction at the nanoscale. We are currently doing some work in this direction.

Acknowledgements

G.A.S., A.A. and J.C. acknowledge the financial support provided by the Basque Country Government (Grant no IT-436-07), the Spanish Ministry of Science and Innovation (Grant no MAT 2007-63681), the Spanish Ministry of Education (Grant no CSD 2006-00053 and PIE 200860I022) and the European Soft Matter Infrastructure. The Donostia International Physics Center (DIPC) financial support is also acknowledged.

References

[1] F. Kremer, A. Schönhals, Broadband Dielectric Spectroscopy, Springer-Verlag, Berlin, 2003.
[2] L. Fumagalli, G. Ferrari, M. Sampietro, G. Gomila, Dielectric-constant measurement of thin insulating films at low frequency by nanoscale capacitance microscopy, Appl. Phys. Lett. 91 (2007) 243110.
[3] G. Gomila, J. Toset, L. Fumagalli, Nanoscale capacitance microscopy of thin dielectric films, J. Appl. Phys. 104 (2008) 024315.
[4] C. Riedel, R. Arinero, Ph. Tordjeman, M. Ramonda, G. Lévêque, G.A. Schwartz, D.G. de Oteyza, A. Alegría, J. Colmenero, Determination of the nanoscale dielectric constant by means of a double pass method using electrostatic force microscopy, J. Appl. Phys. 106 (2009) 024315.
[5] C. Riedel, G.A. Schwartz, R. Arinero, Ph. Tordjeman, G. Lévêque, A. Alegría, J. Colmenero, Nanoscale dielectric properties of insulating thin films: from single point measurements to quantitative images, Ultramicroscopy 110 (2010) 634–638.
[6] M. Zhao, X.H. Gu, S.E. Lowther, C. Park, Y.C. Yean, T. Nguyen, Subsurface characterization of carbon nanotubes in polymer composites via quantitative electric force microscopy, Nanotechnology 22 (2010) 225702.
[7] P.S. Crider, M.R. Majewski., J. Zhang, H. Oukris, N.E. Israeloff, Local dielectric spectroscopy of polymer films, Appl. Phys. Lett. 91 (2007) 013102.
[8] P.S. Crider, M.R. Majewski, J. Zhang, H. Oukris, N.E. Israeloff, Local dielectric spectroscopy of near-surface glassy polymer dynamics, J. Chem. Phys. 128 (2008) 044908.
[9] C. Riedel, R. Sweeney, N.E. Israeloff, R. Arinero, G.A. Schwartz, A. Alegría, Ph. Tordjeman, J. Colmenero, Imaging dielectric relaxation in nanostructured polymers by frequency modulation electrostatic force microscopy, Appl. Phys. Lett. 96 (2010) 213110.
[10] M. Labardi, D. Prevosto, K.H. Nguyen, S. Capaccioli, M. Lucchesi, P. Rolla, Local dielectric spectroscopy of nanocomposite materials interfaces, J. Vac. Sci. Technol. B. 28 (2010). doi:10.1116/1.3368597.
[11] S. Magonov, J. Alexander, Single-pass Kelvin force microscopy and dC/dZ measurements in the intermittent contact: applications to polymer materials, Beilstein J. Nanotechnol. 2 (2011) 15–27.
[12] G.A. Schwartz, E. Tellechea, J. Colmenero, A. Alegría, Correlation between temperature–pressure dependence of the α-relaxation and configurational entropy for a glass-forming polymer, J. Non-Cryst. Sol. 351 (2005) 2616–2621.
[13] J.M. O' Reilly, The effect of pressure on glass temperature and dielectric relaxation time of polyvinyl acetate, J. Poly. Sci. 57 (1962) 429–444.
[14] M. Tyagi, J. Colmenero, A. Alegría, Heterogeneous dynamics of poly(vinyl acetate) far above Tg: a combined study by dielectric spectroscopy and quasielastic neutron scattering, J. Chem. Phys. 122 (2005) 244909.
[15] L. Portes, M. Ramonda, R. Arinero, P. Girard, New method for electrostatic force gradient microscopy observations and Kelvin measurements under vacuum, Ultramicroscopy 107 (2007) 1027–1032.
[16] C. Riedel, J.J. Saenz, Private communication.